5. P. J. Best and R. F. Thompson, *Soc. Neurosci. Abstr.* **10**, 125 (1984).
6. S. E. Fox and J. B. Ranck, Jr., *Exp. Neurol.* **49**, 299 (1975); T. C. Foster *et al.*, *Brain Res.* **408**, 86 (1987).
7. B. H. Bland, P. Andersen, T. Ganes, O. Sveen, *Exp. Brain Res.* **38**, 205 (1980); G. Buzsaki, L. S. Leung, C. H. Vanderwolf, *Brain Res. Rev.* **6**, 139 (1983).
8. B. L. McNaughton, C. A. Barnes, J. O'Keefe, *Exp. Brain Res.* **52**, 41 (1983).
9. Motor set is used in the general sense of preparedness for a particular movement [E. V. Evarts, Y. Shinoda, S. P. Wise, *Neurophysiological Approaches to Higher Brain Functions* (Wiley, New York, 1984)].
10. Stereotrodes [B. L. McNaughton, J. O'Keefe, C. A. Barnes, *J. Neurosci. Methods* **8**, 391 (1983)] consisted of two closely spaced (20 μm) wires. Up to five cells at different distances from the two tips were discriminated at one time by their signal amplitude ratios on the two channels.
11. Unit data were collected as animals traversed a raised platform. On-line analysis identified the location of maximum discharge, that is, the "place field." Event flags inserted into the data stream marked corresponding spatial location for computation of spatial specificity scores. The EEG was filtered, digitized, and stored for off-line Fourier analysis. Mean firing rates for each location, for eight repetitions of each treatment condition, were used to calculate specificity scores. The mean rate in the neutral location was subtracted from the mean rate in the place field, and this difference was divided by the sum of the two means. Treatment effects were assessed by one-way analysis of variance. Location of units in the CA1 region was verified by histology.
12. C. H. Vanderwolf, *Electroencephalogr. Clin. Neurophysiol.* **26**, 407 (1969); R. Kramis, C. H. Vanderwolf, B. H. Bland, *Exp. Neurol.* **49**, 58 (1975).
13. R. U. Muller, J. L. Kubie, J. B. Ranck, Jr., *J. Neurosci.* **7**, 1935 (1987).
14. S. J. Y. Mizumori, B. L. McNaughton, C. A. Barnes, *J. Neurosci.*, in press.
15. D. Gaffan, *Philos. Trans. R. Soc. London Ser. B.* **308**, 87 (1985); N. M. Rupniak and D. Gaffan, *J. Neurosci.* **7**, 2331 (1987).
16. B. L. McNaughton, *Neurosci. Lett.* **29**, S143 (1987); in *Neural Connections and Mental Computations*, L. Nadel, L. Cooper, P. Culicover, R. Harnish, Eds. (Academic Press, New York, 1989), pp. 285–350.
17. E. Halgren, T. L. Babb, P. H. Crandall, *Electroencephalogr. Clin. Neurophysiol.* **45**, 585 (1987).
18. We thank C. A. Barnes for assistance and comments. Supported by PHS grants NS20331 and T32-HD07288.

26 January 1989; accepted 18 April 1989

Activation of Salivary Secretion: Coupling of Cell Volume and $[Ca^{2+}]_i$ in Single Cells

J. KEVIN FOSKETT* AND JAMES E. MELVIN†

High-resolution differential interference contrast microscopy and digital imaging of the fluorescent calcium indicator dye fura-2 were performed simultaneously in single rat salivary gland acinar cells to examine the effects of muscarinic stimulation on cell volume and cytoplasmic calcium concentration ($[Ca^{2+}]_i$). Agonist stimulation of fluid secretion is initially associated with a rapid tenfold increase in $[Ca^{2+}]_i$ as well as a substantial cell shrinkage. Subsequent changes of cell volume in the continued presence of agonist are tightly coupled to dynamic levels of $[Ca^{2+}]_i$, even during $[Ca^{2+}]_i$ oscillations. Experiments with Ca^{2+} chelators and ionophores showed that physiological elevations of $[Ca^{2+}]_i$ are necessary and sufficient to cause changes in cell volume. The relation between $[Ca^{2+}]_i$ and cell volume suggests that the latter reflects the secretory state of the acinar cell. Agonist-induced changes in $[Ca^{2+}]_i$, by modulating specific ion permeabilities, result in solute movement into or out of the cell. The resultant cell volume changes may be important in modulating salivary secretion.

SALIVARY FLUID SECRETION IS NORMALLY initiated by reflex parasympathetic stimulation of the acinar cells (*1*). Intracellular Ca^{2+} ($Ca^{2+}{}_i$) is believed to be the primary regulator of salivary fluid secretion (*1, 2*). Elevation of $[Ca^{2+}]_i$ is thought to stimulate secretion by activating ion permeabilities. Specific Ca^{2+}-sensitive K^+ channels (*3*) and Cl^- currents (*4*) have been identified by patch-clamp techniques in plasma membranes from salivary gland acinar cells. The early phase of stimulation is associated with large net movements of Cl^- (*5–7*) and K^+ (*8*) out of acinar cells. Osmotic consequences of such ion fluxes would have important implications because cell water content affects ion activities, thereby influencing the driving forces for secretion, and rapid alterations of cell size may modulate specific ion channel activities via cell volume-sensing mechanisms (*9*). By simultaneous optical determinations of cell volume and $[Ca^{2+}]_i$ during stimulation of single salivary gland acinar cells, we show that stimulus-secretion coupling in these cells is associated with rapid changes in cell volume, which appear to reflect the secretory state of the cell; the volume changes are shown to be caused by and tightly coupled to dynamic changes in $[Ca^{2+}]_i$.

Carbachol (10 μ*M*) caused a rapid rise of $[Ca^{2+}]_i$, as well as a substantial cell shrinkage (Fig. 1). $[Ca^{2+}]_i$ rose from a resting level of 59 ± 4 n*M* ($n = 62$) to 474 ± 50 n*M* ($n = 31$) within 3 s. Shrinkage was first detected close to the time that $[Ca^{2+}]_i$ reached peaked levels (Fig. 1A). Even though the $[Ca^{2+}]_i$ increase usually began to subside during the next 15 to 30 s, the cells continued to shrink, reaching a minimum volume at 10 to 30 s after the initial rise of $[Ca^{2+}]_i$. Maximum volume loss was 15% ± 1% ($n = 25$).

After the initial spike, the response of $[Ca^{2+}]_i$ to the continued presence of carbachol varied among cells. Generally, $[Ca^{2+}]_i$ remained considerably higher than resting levels for as long as the agonist was present (Fig. 1, B and C). Removal of carbachol caused $[Ca^{2+}]_i$ to return rapidly to resting levels (Fig. 1, B and C). In some cells, $[Ca^{2+}]_i$ returned close to resting levels within 5 min in the continued presence of carbachol (Fig. 1D). Despite this variability among cells in the level and kinetics of the sustained phase of the $[Ca^{2+}]_i$ response, cell volume was correlated with $[Ca^{2+}]_i$ in all cases. Thus, sustained elevated $[Ca^{2+}]_i$ was associated with sustained shrinkage (Fig. 1B); $[Ca^{2+}]_i$ relaxation to intermediate levels was associated with the recovery of cell volume to intermediate levels (Fig. 1C), and transiently elevated $[Ca^{2+}]_i$ was associated with shrinkage followed by volume recovery (Fig. 1D).

Secretagogues raise $[Ca^{2+}]_i$ by mobilizing Ca^{2+} from intracellular stores (*10*), possibly the endoplasmic reticulum (*11*) associated with the basolateral membrane (*12*), as well as by enhancing plasma membrane Ca^{2+} permeability (*10*). In the presence of agonist and extracellular Ca^{2+} ($Ca^{2+}{}_o$), Ca^{2+} entry resulted in a sustained elevation of $[Ca^{2+}]_i$ in most of the acinar cells examined (Fig. 1, B and C). In the absence of $Ca^{2+}{}_o$, stimulation was associated with a peak $[Ca^{2+}]_i$ (712 ± 115 n*M*), which was comparable ($P = 0.4$) to that observed for cells stimulated in Ca^{2+}-containing medium. However $[Ca^{2+}]_i$ generally returned to resting levels within 3 min as intracellular stores became depleted (Fig. 2A). Associated with the $[Ca^{2+}]_i$ spike was a rapid cell shrinkage (volume loss, 15% ± 1%) indistinguishable from that observed in Ca^{2+}-containing medium. In cells stimulated in the absence of $Ca^{2+}{}_o$, however, the shrinkage was transient, and the cells recovered their volumes with a time course that was comparable with the recovery of $[Ca^{2+}]_i$ (Fig. 2A). These data indicate that mobilization of $[Ca^{2+}]_i$

J. K. Foskett, Physiology Department, Armed Forces Radiobiology Research Institute, Bethesda, MD 20814. J. E. Melvin, Clinical Investigations and Patient Care Branch, National Institute of Dental Research, National Institutes of Health, Bethesda, MD 20862.

*Present address and to whom correspondence and reprint requests should be addressed at Division of Cell Biology, Research Institute, The Hospital for Sick Children, 555 University Avenue, Toronto, Ontario M5G 1X8, Canada.
†Present address: Department of Dental Research, University of Rochester, Box 611, 605 Elmwood Ave., Rochester, NY 14642.

from intracellular stores is sufficient to cause cell shrinkage, and subsequent cell volume appears to be highly correlated with $[Ca^{2+}]_i$.

To establish further the Ca^{2+}-dependence of the cell volume changes observed during stimulation, we loaded cells with the Ca^{2+}-chelator bis(2-amino-5-methylphenoxy)ethane-*N,N,N*^{1},*N*^{1}-tetra-acetate (dimethyl-BAPTA) and stimulated them in the absence of $Ca^{2+}{}_o$ (Fig. 2B). The $[Ca^{2+}]_i$ response to stimulation is abolished or greatly attenuated under these conditions, although BAPTA-loaded parotid acinar cells retain intact signal transduction mechanisms (*12*). Severe attenuation of the $[Ca^{2+}]_i$ response also abolishes the responses of cell volume to carbachol stimulation (Fig. 2B). These experiments show that elevated $[Ca^{2+}]_i$ is necessary to initiate the volume changes observed with stimulation. To test whether a rise of $[Ca^{2+}]_i$ is in itself sufficient to trigger shrinkage, we used the Ca^{2+} ionophore ionomycin to raise $[Ca^{2+}]_i$, bypassing receptor-mediated transduction mechanisms. Ionomycin (3 μ*M*) caused a moderately rapid rise of $[Ca^{2+}]_i$ to levels (>5 μ*M*) that saturate fura-2 (Fig. 2C). The early part of this time course is associated with a rapid cell shrinkage similar to that observed with agonist stimulation. However, this shrinkage was followed by a rapid volume recovery despite high $[Ca^{2+}]_i$. Cell volume may have a biphasic dose dependency on $[Ca^{2+}]_i$ such that supra-physiological levels of $[Ca^{2+}]_i$ exert another effect, which causes the cells to swell. To test this, cells were continuously exposed to 0.5 μ*M* ionomycin, which is sufficient to transiently elevate $[Ca^{2+}]_i$ to levels reached during agonist stimulation (Fig. 2D). The cells were periodically exposed to 5- to 15-s pulses of 3 μ*M* ionomycin to maintain elevated $[Ca^{2+}]_i$ at approximately this level (Fig. 2D). The results indicate that an increase in $[Ca^{2+}]_i$ is associated with cell shrinkage so long as $[Ca^{2+}]_i$ is within normal physiological levels.

An additional observation demonstrates that cell volume is tightly coupled to physiological levels of $[Ca^{2+}]_i$. Although the kinetics of $[Ca^{2+}]_i$ during agonist stimulation are usually as shown in Fig. 1, occasionally (10 of 31 cells) carbachol triggers damped $[Ca^{2+}]_i$ oscillations with a period of ~5 min. These $[Ca^{2+}]_i$ oscillations are associated with similar oscillations in cell volume (Fig. 3A). With the exception of the earliest several seconds of stimulation (since the initial rise of $[Ca^{2+}]_i$ precedes any change in volume), cell volume is linearly related to $[Ca^{2+}]_i$ during this entire oscillatory period (Fig. 3B).

Our results show that a rapid change in cell volume is an early event associated with stimulus-secretion coupling in parotid salivary acinar cells. This time course of the rapid shrinkage associated with the initial agonist-induced rise of $[Ca^{2+}]_i$ is similar to that of Cl^- loss (*5, 7*) measured in cell suspensions. Since most biological membranes have a high water permeability, volume changes reflect changes in solute content of the cells. Thus, the rapid shrinkage associated with stimulation most likely reflects predominantly a KCl loss from the cell due to agonist-enhanced plasma membrane K^+ and Cl^- conductances. Simultaneous measurements of intracellular Cl^- activity (with a Cl^--sensitive fluorescent dye) and the volume of single cells support this hypothesis (*13*).

The Ca^{2+} dependence of the response of cell volume to stimulation is reminiscent of the $Ca^{2+}{}_o$-dependence of salivary secretion. Thus, stimulation in either Ca^{2+}-containing or Ca^{2+}-free medium elicits similar initial membrane permeability changes, ion effluxes, and increases in $[Ca^{2+}]_i$ (*14*), but only in the presence of $Ca^{2+}{}_o$ are these indices of secretion in vitro as well as secretion in vivo (*15*) sustained. This similarity of the $Ca^{2+}{}_o$ dependencies of cell volume and salivary secretion suggests that volume may be a useful indicator of the secretory state of the acinar cell. After the initial shrinkage, subsequent volume changes are tightly linked to subsequent changes in $[Ca^{2+}]_i$. Cell swelling associated with relaxation of $[Ca^{2+}]_i$ toward resting levels indicates that volume restorative mechanisms (that is, solute influx) must also be activated by carbachol. Because cell volume reflects the balance between salt influx and efflux rates,

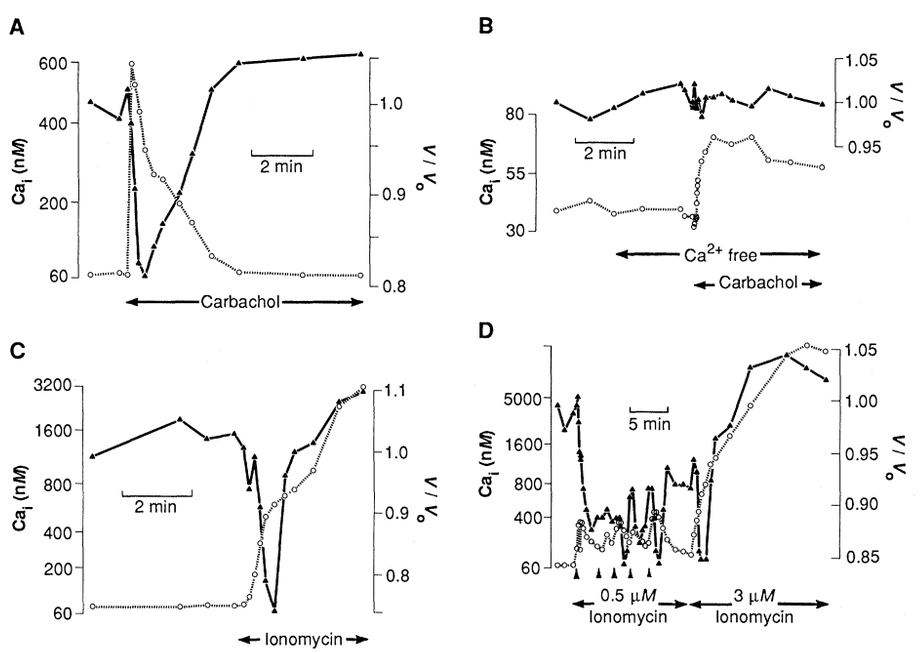

Fig. 1. Time courses of $[Ca^{2+}]_i$ (○) and cell volume (▲). In each experiment, a single acinar cell was stimulated with 10 μ*M* carbachol. Cell volume (*V*) is shown as a fraction of original volume (V_o). (**A**) High temporal resolution to demonstrate the rates and relations of $[Ca^{2+}]_i$ and cell volume changes. (**B** to **D**) Variability among cells in the responses of $[Ca^{2+}]_i$ and volume to prolonged exposure to carbachol. Single rat parotid acinar cells were loaded with fura-2 (Molecular Probes) and perfused continuously (37°C, 5% CO_2) on the stage of an inverted microscope (*7, 12, 19*). Single cells were viewed simultaneously in differential interference contrast (DIC) and fluorescence optics (*19*). Fluorescence images (excitation 340 n*M* and 390 n*M*; emission 510 nm) were background-subtracted and divided on a pixel by pixel (256 × 240) basis to generate spatially resolved maps of $[Ca^{2+}]_i$ with 800-ms resolution. $[Ca^{2+}]_i$ was determined by integrating pixel intensities throughout the cell. Fluorescence ratios were converted to $[Ca^{2+}]_i$ by calibrations of a separate group of cells and of fura-2–free acid in 20-μm-thick glass capillaries, with similar results. Fura-2–loaded cells were incubated for 60 to 90 min in Ca^{2+}-free medium containing 20 μ*M* dimethyl-BAPTA acetoxymethyl ester to lower $[Ca^{2+}]_i$ to close to zero. After determination of the ratio of the unbound form of fura-2 (R_{min}) cells were exposed to Ca^{2+} and 3 μ*M* ionomycin to rapidly elevate $[Ca^{2+}]_i$ to levels that saturate the dye (R_{max}). $[Ca^{2+}]_i = \beta K_d [(R - R_{min})/(R_{max} - R)]$ where K_d (the dissociation constant of the dye) was assumed to be 220 n*M* and β is the ratio of fluorescence at 390 n*M* excitation for fura-2 (unbound) to fura-2 (bound) (*20*). A video disk recorder coupled to a second video camera captured the DIC image of the same cell synchronously with the digitization of the fluorescence images. Individual acinar cells are essentially spherical when isolated onto cover slips as described. Volume changes are associated (to a first approximation) with equal changes in the size of the cell in all three dimensions (not shown). Planimetry of the images of a cell obtained at a constant optical section provided a time course of its area throughout the experiment. Cell volume changes were estimated by raising area changes to the 3/2 power.

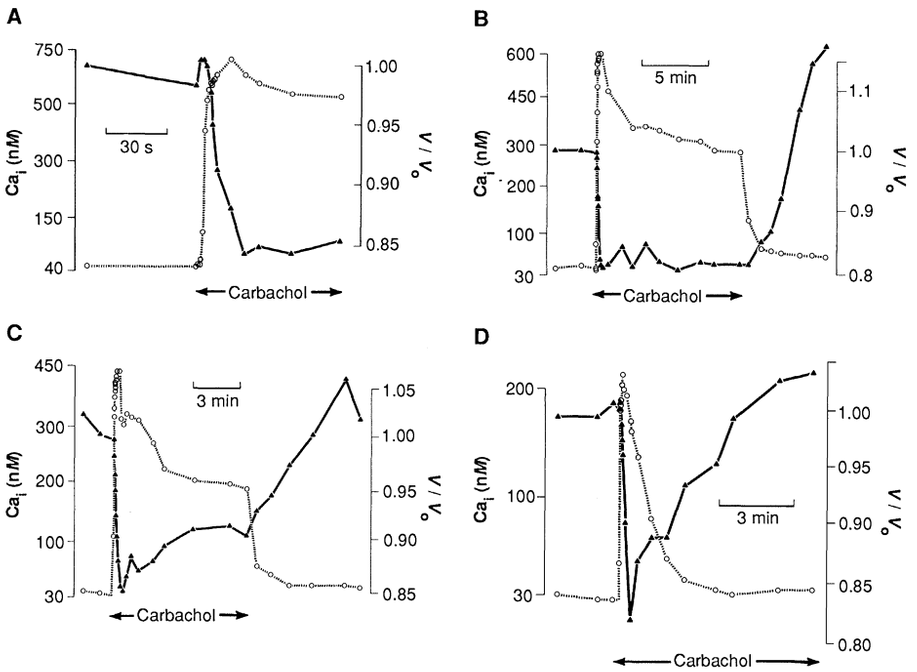

Fig. 2. Time course of single cell $[Ca^{2+}]_i$ (○) and volume (▲) during stimulation with 10 μ*M* carbachol (A and B) or ionomycin (C and D). (**A**) Cell stimulated in the absence of extracellular Ca^{2+}; (**B**) BAPTA-loaded cell; (**C**) 3 μ*M* ionomycin; (**D**) 0.5 μ*M* ionomycin; at arrowheads, 3 μ*M* ionomycin was perfused through the chamber for 5 to 15 s. Resultant fluctuations of $[Ca^{2+}]_i$ within the physiological range cause similar fluctuations of cell volume. EGTA (1 m*M*) replaced the Ca^{2+} in Ca^{2+}-free medium. BAPTA loading of cells was accomplished by first loading the cells with fura-2, as described, then incubating the cells for an additional 60 min in 15 μ*M* of the permeant acetoxymethyl ester of dimethyl-BAPTA (K_d = 40 n*M*) (*21*) (Molecular Probes) under identical conditions (*12*).

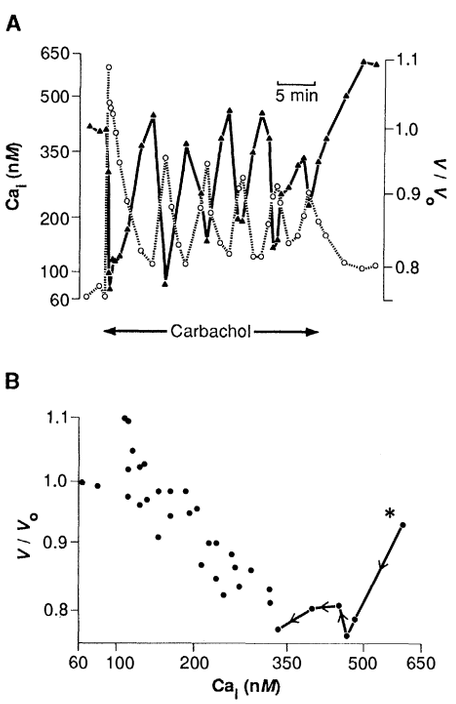

Fig. 3. (**A**) Carbachol (10 μ*M*)–induced oscillations of single cell $[Ca^{2+}]_i$ (○) and volume (▲). (**B**) Correlation of $[Ca^{2+}]_i$ and volume during carbachol-induced oscillations. The asterisk indicates the first data obtained after stimulation; the line connects subsequent data in correct temporal sequence, demonstrating that during the initial phases of stimulation $[Ca^{2+}]_i$ rises before the cell shrinks. Subsequently, during the oscillatory phase, the ratio 340/390 and cell volume are linearly related.

sustained cell shrinkage indicates that solute influx and efflux rates are exactly balanced (after the initial KCl loss). Since known Cl^- influx pathways are localized in the basolateral membrane (*1, 16*), such a balance would result in sustained fluid secretion. These data suggest that sustained cell shrinkage during sustained elevated $[Ca^{2+}]_i$ reflects sustained fluid secretion. To the extent that $[Ca^{2+}]_i$ returns toward resting levels, the cells swell correspondingly toward control levels (Fig. 1), indicating that solute influx rates exceed those for solute efflux. When $[Ca^{2+}]_i$ returns toward resting levels, the probabilities that the K^+ and Cl^- channels are open decrease (*2, 3*). A reduced KCl permeability reduces the rate of fluid secretion. Thus, to the extent that apical Cl^- or basolateral K^+ (or both) conductances are reduced, both the shrinkage and the rate of fluid secretion are reduced proportionately. Thus, cell volume under these conditions also appears to reflect the secretory state of the cell.

Regardless of the specific ionic mechanisms underlying them, agonist-induced volume changes may regulate salivary secretion. Changes in cell volume alter ion activities and thereby directly affect the electrochemical driving forces for fluid secretion. Furthermore, cell volume changes may alter specific membrane transport properties (*9*).

The results of our study demonstrate agonist-induced changes in cell volume. We observed similar cell volume changes in single acini and acinar clumps (*17*). Stimulation of intact salivary glands in vivo is associated with a reduction in intracellular space (*18*), indicating that the observed volume changes in single cells are representative of events in vivo. Our results demonstrate a direct link between the activity of an intracellular messenger and cell volume. It will be of interest to examine whether stimulation-associated elevations of $[Ca^{2+}]_i$ or activation of ion transport pathways in other cell types is also associated with changes in cell volume.

REFERENCES AND NOTES

1. J. A. Young, D. I. Cook, E. W. van Lennap, M. Roberts, in *Physiology of the Digestive Tract*, L. R. Johnson, Ed. (Raven Press, New York, 1987), pp. 773–815.
2. O. H. Petersen, *Am. J. Physiol.* **251**, GI (1986); ____ and Y. Maruyama, *Nature* **307**, 693 (1984); J. W. Putney, Jr., *Pharm. Rev.* **30**, 209 (1979); *Annu. Rev. Physiol.* **48**, 75 (1986).
3. Y. Maruyama, D. V. Gallacher, O. H. Petersen, *Nature* **302**, 827 (1983).
4. N. Iwatsuki, Y. Maruyama, O. Matsumoto, A. Nishiyama, *Jpn. J. Physiol.* **35**, 933 (1985).
5. B. Nauntofte and J. H. Poulsen, *Am. J. Physiol.* **251**, C175 (1986).
6. I. S. Ambudkar, J. E. Melvin, B. J. Baum, *Pfluegers Arch.* **412**, 75 (1988); J. R. Martinez and N. Cassity, *ibid.* **403**, 50 (1985); J. R. Martinez, *J. Dent. Res.* **66**, 638 (1987).
7. J. E. Melvin, M. Kawaguchi, B. J. Baum, R. J. Turner, *Biochem. Biophys. Res. Commun.* **145**, 754 (1987).
8. J. A. Mangos, N. R. McSherry, T. Barber, *Am. J. Physiol.* **229**, 566 (1975); J. H. Poulson and S. W. Bledsoe, *ibid.* **234**, E79 (1978); J. H. Poulsen and B. Oakley II, *Proc. R. Soc. London Ser. B* **204**, 99 (1979).
9. J. L. Eveloff and D. G. Warnock, *Am. J. Physiol.* **252**, F1 (1987); H. Sackin, *ibid.* **253**, F1253 (1987); O. Christensen, *Nature* **330**, 66 (1987); R. L. Hudson and S. G. Schultz, *Proc. Natl. Acad. Sci. U.S.A.* **85**, 279 (1988).
10. D. L. Aub and J. W. Putney, Jr., *J. Dent. Res.* **66**, 547 (1987); J. W. Putney, Jr., D. L. Aub, C. W. Taylor, J. E. Merritt, *Fed. Proc.* **45**, 2634 (1986); J. E. Merritt and T. J. Rink, *J. Biol. Chem.* **262**, 4958 (1987); B. Nauntofte and S. Dissing, *Am. J. Physiol.* **253**, G290 (1987); J. Poggioli and J. W. Putney, Jr., *Pfluegers Arch.* **392**, 239 (1982); H. R. Koelz, S. Kondo, A. L. Blum, I. Schulz, *ibid.* **370**, 37 (1977); B. E. Miller and D. L. Nelson, *J. Biol. Chem.* **252**, 3269 (1977); J. Poggoli, S. J. Weiss, J. S. McKinney, J. W. Putney, Jr., *Mol. Pharm.* **23**, 71 (1983).
11. D. Boms, D. Giraud, B. Rossignol, *Biol. Cell* **57**, 271 (1986); V. Henne, A. Puper, H.-O. Soling, *FEBS Lett.* **218**, 153 (1987).
12. J. K. Foskett, P. J. Gunter-Smith, J. E. Melvin, R. J. Turner, *Proc. Natl. Acad. Sci. U.S.A.* **86**, 167 (1989).
13. J. K. Foskett, *FASEB J.* **3**, A982 (1989).
14. O. H. Petersen, J. H. Poulsen, N. A. Thorn, *Acta Physiol. Scand.* **71**, 203 (1967); O. H. Petersen and G. L. Pedersen, *J. Membr. Biol.* **16**, 353 (1974); J. W. Putney, Jr., *Cell Calcium* **4**, 439 (1983); J. R. Martinez and N. Cassity, *Pfluegers Arch.* **407**, 615 (1986); M. K. McMillian, S. P. Soltoff, L. C. Cantley, B. R. Talamo, *Biochem. Biophys. Res. Commun.* **149**, 523 (1987); J. E. Merritt and T. J. Hallam, *J. Biol. Chem.* **263**, 6161 (1988); J. E.

Merritt and T. J. Rink, *ibid.* **262**, 14912 (1987); *ibid.*, p. 4592; *ibid.*, p. 17362.
15. W. W. Douglas and A. M. Poisner, *J. Physiol. (London)* **165**, 528 (1963).
16. R. J. Turner, *Am. J. Physiol.* **254**, C391 (1988); M. Manganel and R. J. Turner, *J. Membr. Biol.* **102**, 247 (1988).
17. Carbachol-induced shrinkage was similar in single cells, single acini, or acinar clumps. However, subsequent volume changes in acini and acinar clumps could differ from those observed in single cells, depending on the availability of Ca^{2+}_o. In the absence of Ca^{2+}_o, subsequent volume recovery was observed in acini and acinar clumps that was similar to that observed in single cells. In the presence of Ca^{2+}_o, however, stimulation of acini and acinar clumps was associated with the development of large fluid-filled vacuoles. These vacuoles were not observed in single cells, suggesting that they might represent trapped extracellular fluid. Determination of cell volume as described in this study is questionable when vacuoles develop. Therefore, data are from single cells only, where these vacuoles do not contribute to the volume determinations.
18. A. S. V. Burgen and N. G. Emmelin, *Physiology of the Salivary Glands* (Arnold, London, 1961).
19. J. K. Foskett, *Am. J. Physiol.* **255**, C566 (1988).
20. G. Grynkiewicz, N. M. Poenie, R. Y. Tsien, *J. Biol. Chem.* **260**, 3440 (1985).
21. R. Y. Tsien, *Biochemistry* **19**, 2396 (1980).
22. Supported by the Armed Forces Radiobiology Research Institute, Defense Nuclear Agency, under research work unit B0156. The views presented in this paper are those of the authors. No endorsement by the Defense Nuclear Agency has been given or should be inferred.

9 January 1980; accepted 21 April 1989

Production of Mammastatin, a Tissue-Specific Growth Inhibitor, by Normal Human Mammary Cells

P. R. ERVIN, JR., M. S. KAMINSKI, R. L. CODY, M. S. WICHA*

The growth of human mammary cells may be regulated by a balance between growth stimulatory and growth inhibitory pathways. Polypeptides of 47 and 65 kilodaltons (mammastatin) were isolated from conditioned medium of normal human mammary cells. Monoclonal antibodies against mammastatin were generated that blocked its activity and were used for purification and further characterization of the protein. Mammastatin inhibited the growth of 5 transformed human mammary cell lines, but had no effect on the growth of 11 transformed human cell lines derived from nonmammary tissues. Mammastatin appeared to be a heat-labile protein distinct from transforming growth factor–β (TGF-β). By immunoperoxidase staining it was detected in cultured normal human mammary cells, but was decreased in transformed mammary cells.

MAMMARY EPITHELIAL CELLS have provided a particularly useful model to study growth control mechanisms. Both in vitro and in vivo mammary epithelial growth is regulated by steroid hormones and polypeptide growth factors (*1*). Steroid hormones such as estrogen may influence cell proliferation by stimulating the autocrine or paracrine release of positive growth regulators such as TGF-α and insulin-like growth factor 1, as well as by inhibiting the production of negative growth regulators such as TGF-β (*2, 3*). The polypeptide growth factors involved in these pathways do not have cell type specificity, but are capable of affecting the growth of a wide variety of cell types in culture (*4, 5*). In contrast to these nonspecific inhibitors, we have postulated that mammary tissue–specific polypeptide growth factors should exist that are analogous to mullerian inhibitory substance, which selectively inhibits the growth of the mullerian duct in the male embryo (*6, 7*).

Division of Hematology and Oncology, Department of Internal Medicine, University of Michigan Cancer Center, Ann Arbor, MI 48109.

*To whom correspondence should be addressed.

Normal human mammary cells (NHMC), characterized as epithelial by keratin expression, were derived from reduction mammoplasties and serially passaged in low calcium medium (<60 n*M*) (*8*). Media conditioned by these cells was found to inhibit the growth of the transformed human mammary carcinoma cell line, MCF-7, in a time and dose-dependent manner (Fig. 1). The addition of 10% conditioned medium (concentrated ten times by ultrafiltration) to these cultures resulted in a 75% inhibition of cell growth at 10 days compared to cultures supplemented with 10% nonconditioned medium.

To purify and further characterize the factor, or factors, from conditioned medium responsible for growth inhibition, we used a combination of ion-exchange and molecular sieve chromatography (Table 1). Fractions were analyzed for growth inhibitory activity on MCF-7 cells. By ion-exchange chromatography on a DEAE column eluted with a

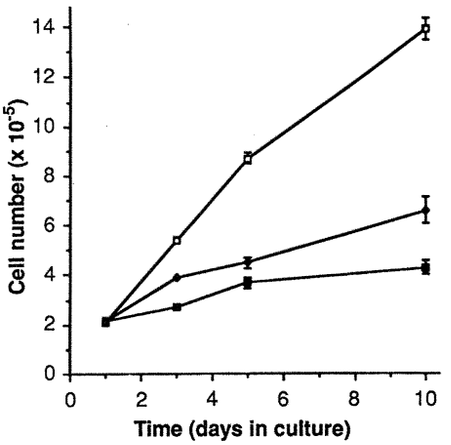

Fig. 1. Effect of conditioned medium on MCF-7 gorwth. MCF-7 cells were plated at 2×10^5 cells per T25 flask in Dulbecco's minimum essential medium (DMEM) with 10% fetal calf serum and insulin (10 μg/ml) and allowed to attach overnight. Medium was then replaced with indicated concentration of conditioned medium produced by incubating confluent cultures of NHMC for 4 days in DMEM–F-12, at 40 n*M* $CaCl_2$ with 5% chelex-treated bovine serum. Conditioned or nonconditioned medium was concentrated 10× by Amicon ultrafiltration. Cell number was determined at indicated times by Coulter counting. □, Ten percent nonconditioned medium; ◆, 5% conditioned medium; ■, 10% conditioned medium. Values represent mean ± SEM of triplicate determinations repeated twice.

Table 1. Purification of mammastatin. The inhibitory activity in NHMC-conditioned medium was purified by ion-exchange chromatography on DEAE Sephacryl followed by affinity chromatography on a 3C6 monoclonal antibody affinity column. One liter of conditioned medium was loaded on a DEAE column in 50 m*M* NaCl and eluted with a step gradient between 0.05 and 1.0*M* NaCl. Dialyzed fractions were assayed for MCF-7 growth inhibitory activity. Fractions exhibiting inhibitory activity, which eluted between 0.1 and 0.5*M* NaCl, were passed over an affinity column produced by binding 22 mg of 3C6 monoclonal antibody to 1.5 ml of Bio-Rad Affi-Gel Beads. The affinity column was washed with 500 column volumes of PBS, and bound protein was eluted with 0.5*M* glycine, *p*H 2.35. The eluent was neutralized with tris base and dialyzed against PBS. Specific activity is defined in units per milligram, where one unit is the amount of protein necessary to produce 50% inhibition of MCF-7 cell growth. Concentration of the inhibitory protein was determined by comparison with albumin standards on SDS-PAGE gels visualized by silver stain. Final purity of the inhibitory proteins was determined to be greater than 50%.

Sample	Total protein (mg)	Specific activity	Purification (fold)	Yield (%)
Conditioned media	2,150	1.16	1	100
0.5*M* DEAE fraction	20.3	47.7	41	40.3
Affinity purified	0.0012	106,000.0	91,380	5.3